



Shock Mitigation Studies of Solid Foams for Z-Pinch Chamber Protection

M. Anderson, J. Oakley, V. Vigil, S. Rodriguez, R. Bonazza

September 2005

UWFDM-1281

Presented at the 21st IEEE/NPSS Symposium on Fusion Engineering (SOFE), 26-29
September 2005, Knoxville TN.

FUSION TECHNOLOGY INSTITUTE

UNIVERSITY OF WISCONSIN

MADISON WISCONSIN

DISCLAIMER

This report was prepared as an account of work sponsored by an agency of the United States Government. Neither the United States Government, nor any agency thereof, nor any of their employees, makes any warranty, express or implied, or assumes any legal liability or responsibility for the accuracy, completeness, or usefulness of any information, apparatus, product, or process disclosed, or represents that its use would not infringe privately owned rights. Reference herein to any specific commercial product, process, or service by trade name, trademark, manufacturer, or otherwise, does not necessarily constitute or imply its endorsement, recommendation, or favoring by the United States Government or any agency thereof. The views and opinions of authors expressed herein do not necessarily state or reflect those of the United States Government or any agency thereof.

Shock Mitigation Studies of Solid Foams for Z-Pinch Chamber Protection

M. Anderson, J. Oakley, V. Vigil, S. Rodriguez,
R. Bonazza

Fusion Technology Institute
University of Wisconsin
1500 Engineering Drive
Madison, WI 53706

<http://fti.neep.wisc.edu>

September 2005

UWFDM-1281

Presented at the 21st IEEE/NPSS Symposium on Fusion Engineering (SOFE), 26-29 September 2005,
Knoxville TN.

Shock Mitigation Studies of Solid Foams for Z-Pinch Chamber Protection

Mark Anderson^a, Jason Oakley^a, Virginia Vigil^a, Salvador Rodriguez^b, Riccardo Bonazza^a

^a University of Wisconsin-Madison, Madison, Wisconsin, USA

^b Sandia National Laboratory, Albuquerque, New Mexico, USA

Abstract—Solid open-cell Al foams are subjected to dynamic compression testing in a vertical shock tube to model the metallic foam being considered for use in an inertial fusion energy reactor. High porosity (0.89) foam samples (stack of two, 25.4 cm square, 10.2 cm high) of three different cell sizes (10, 20, and 40 pores per inch) are compressed with a strong shock ($M=6$) in a 25 kPa atmosphere of air and SF₆. The post-shock samples are highly compressed (strains up to 0.8 for the smallest cell size) and have a wavy upper surface indicating structural anisotropy. Energy absorption is found to vary with cell size (smaller cells, more absorption) while the impulse of the shock wave is independent of cell size. Pressure data indicate the incident shock wave becomes a compression wave with a non-discontinuous gradient inside of the foam. Using an array of pressure transducers with a vertical spacing of 2.54 cm, the wave speed in the foam sample is reduced to 25% of its value without the presence of the foam.

Keywords - shock mitigation, first-wall protection, solid aluminum foam

I. INTRODUCTION

Inertial fusion energy (IFE) power plant designs require a shock mitigation strategy to protect the chamber from repeated thermonuclear blasts. One proposed idea for a high repetition rate (6 Hz) moderate yield (350 MJ) conceptual power plant design is to use flowing liquid Flibe (F₂LiBe₄), either sheets or jets in a staggered configuration, to protect the walls [1] and also to serve the functions of heat transfer and nuclear fuel breeding. Currently, there is an ongoing conceptual power plant design that instead utilizes high yield reactions (3 GJ) at a much lower rate (0.1 Hz) and this provides a more challenging scenario where shock mitigation becomes more important. This new design utilizing Z-pinch technology [2] is investigating the use of foam(s) to reap the benefits that a two-phase material can provide for shock mitigation [3]. The IFE target is suspended from above in the center of the chamber filled with low pressure gas (10-20 torr), inside of a hohlraum, by a conical recyclable transmission line (RTL). The interior of the RTL will be filled with solid foam Flibe to protect the top of the chamber, while a bubbly pool protects the bottom, and foamed liquid jets and sheets protect the side walls.

Solid aluminum foam may be used as model material while a solid Flibe foam (or PbLi foam) is under development. Previously, a series of low Mach number experiments ($M=1.34$) studied the shock attenuation properties of a single 2.54 cm layer suspended in a shock tube and also the effect of two layers separated by two different spacings [4]. The pressure behind the transmitted shock was reduced by 30%

(compared with the incident shock) while the wave speed was reduced by 10% for the single layer configuration in Ar initially at atmospheric pressure. The two layer configuration resulted in even greater pressure attenuation (50%) while the spacing between the layers was found to have little effect.

The experiments reported here are for a new set of high Mach number experiments ($M=6$) where the objectives are: 1) to study the attenuation of the shock wave as it passes through the foam material, and 2) the energy absorption that occurs during the shock interaction, as well as effects on wave speed and pressure. This data can then be used for initial code calculation verification and validation, before more complex high strength experiments are performed.

II. EXPERIMENT

The Wisconsin Shock Tube Laboratory [5] is utilized to conduct these strongly shocked aluminum foam studies. The 9.2 m long vertical shock tube has a large internal square cross section (25.4 cm sides), and is designed to withstand pressures of 20 MPa. Shock piezoelectric pressure transducers are flush mounted along a vertical wall of the shock tube to measure the transient nature of the pressure and the wave speeds. The driven section of the shock tube is filled with a high molecular weight gas (volume mixture of 20% air and 80% SF₆) at low pressure (25 kPa absolute) in order to obtain a very strong incident shock ($M=6$) with a pressure ratio of 38 and a wave speed of $W_1=956$ m/s. Helium is used in the driver at a pressure of 5.1 MPa.

Figure 1 shows a sample in the bottom of the shock tube in the test section before the side flange is installed. The sample is mounted flush with the shock tube walls and is a stack of two 10.2 cm high samples setting on a rigid, 6.35 cm thick, solid Al plate. There is an ink grid on each side of the sample with squares having 2.54 cm sides to assist in visualizing the deformation post-shock. Pressure transducers are vertically spaced at 2.54 cm in the test section and also placed beneath the foam in the bottom flange. The test begins by installing the side wall flange for the test section, evacuating the driven section to 5 kPa of air, filling to 25 kPa with SF₆, overpressurizing the driver with He to 5.1 MPa, thereby releasing the shock wave.

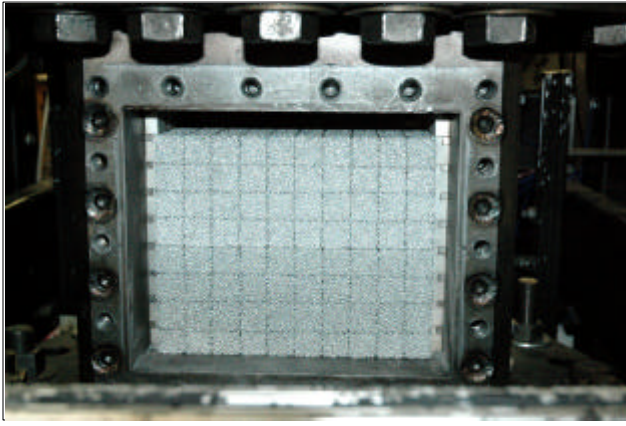


Figure 1. Test section of shock tube showing Al foam sample installed.

III. ALUMINUM FOAM MATERIAL

Metallic foams have been used in a variety of applications, including: compact heat exchangers, filters, and lightweight structural support [6]. The material is open-cell Al foam manufactured by ERG [7] with cell morphology shown in Fig. 2. Foam samples with three different linear cell sizes, 2.54, 1.27, and 0.64 mm, were tested and are referred to as 10, 20, and 40 ppi (pores per inch). The porosity is defined as $f = 1 - \frac{r_c}{r_s}$ where the solid Al 6061 T6 density is $r_s = 2,700 \text{ kg/m}^3$ and the cellular density is nominally $r_c = 0.08r_s$, but measured to be $r_c = 0.11r_s$. Although the cell size in the three experiments varied, and in turn the connecting ligament diameter, the porosity for all samples was a constant $f = 0.89$. The compressive yield strength for 40 ppi foam with this porosity has a plateau of $S_{yc} = 3.0 \text{ MPa}$ and is relatively independent of the pore size [8].

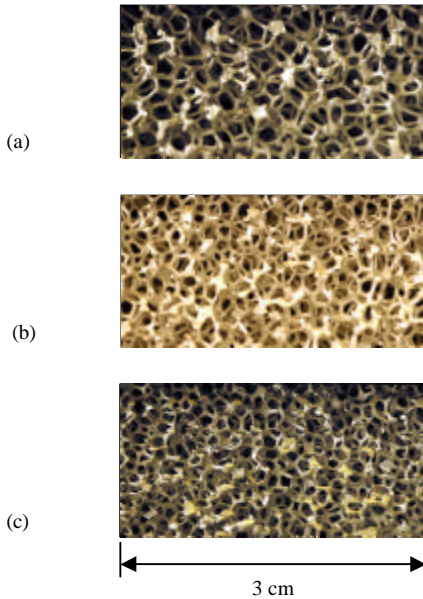


Figure 2. Open cell-cell morphology as a function of pore size: (a) 10 ppi, (b) 20 ppi, (c) 40 ppi.

IV. RESULTS

Prior to testing the samples, a series of calibration runs were conducted to quantify the shock wave and verify the operability of the pressure transducers. The data collected during the shocked foam experiments were sample compression and topology, and pressure traces.

A. Layer compression and surface topology

Figure 3 shows the post-shock results of the samples after they were removed from the shock tube. Although the incident shock wave is planar and parallel to the top surface of the sample, and therefore initially provides uniform surface compression, the samples have deformed in an anisotropic fashion noted by the wavy surface evident in Fig. 3. SEM micrographs from previous studies [9] have shown some anisotropy in the cast Al foam, solidification versus transverse direction, resulting in variations in the yield strength of 5-10% [8] depending on the direction of the applied elastic compression. The resulting wavy nature of the foam surface indicates that there may be regions of anisotropy that are not simply related to the direction of solidification. The larger pore size samples (10 and 20 ppi) experienced compression purely by yielding; however, the 40 ppi sample experienced a fracture which indicates part of the sample had been locally strained to beyond plateau compressive yield stress. The top surface topology was measured with a Perceptron® laser scanner and the contour plots are shown in Fig. 4. The largest pore size (10 ppi) experienced the least compression because it provides the least resistance to the passage of the shock wave, analogous to its performance as a filter in incompressible flows where the pressure drop is less than the 20 ppi sample. Contour lines on each of the plots indicate surface feature sizes (valleys, peaks, etc.) on the order of 5-10 cm which is larger than the samples typically used in compressive yield tests [8,9] so these large sample shock tube tests may indicate an anisotropic material response not previously observed.

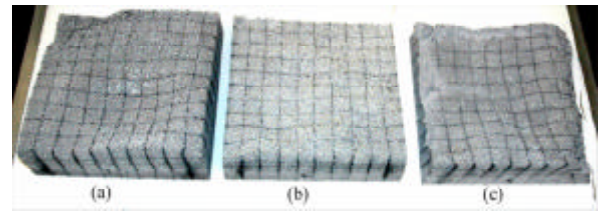


Figure 3. Post-shocked foam samples: (a) 10 ppi, (b) 20 ppi, (c) 40 ppi.

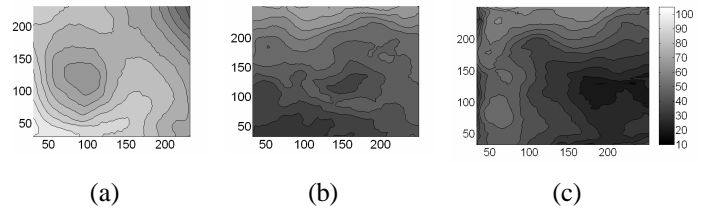


Figure 4. Contours of post-shocked foam samples: (a) 10 ppi, (b) 20 ppi, (c) 40 ppi. Dimensions in mm.

Energy absorption of the foam samples can be determined by measuring the strain of the post-shocked samples. The area under the stress-strain curve is an indication of “work per unit volume”, therefore:

$$E_{abs} \approx s_{yc} \bar{\epsilon} V_0 \quad ,$$

where E_{abs} is the energy absorbed by the Al foam, $\bar{\epsilon} = 1 - h/h_0$ is the average strain, and V_0 is the initial volume. Calculation results are given in Table I using the initial height of the samples, $h_0 = 203.2$ mm and $V_0 = 0.0131$ m³. There is a much larger increase in absorbed energy when the pore size is halved from the 10 ppi sample to the 20 ppi sample and a much smaller increase is observed from the 20 to 40 ppi. The measured absorbed energy from these samples is on the order of 30 kJ, which is a factor of 20 less than the energy absorbed in the conceptual reactor design (5 m radius chamber, 3 GJ yield, results in a 620 kJ deposition of energy on a 0.0645 m² area- the area of the tested Al foam sample.) However, in the reactor, the foam nearest the center of the chamber will vaporize due to thermal energy absorption; this will result in an ablation and a hydrodynamic shock that travels through the RTL. With an advanced radiation-hydrodynamics code, the energy can be examined in more detail and it may show that the energy absorption at the outer radius of the chamber is much closer to the 30 kJ range because of heating, vaporization, ablation, and other effects that will aid in attenuating the energy before it reaches the chamber wall.

TABLE I. ENERGY ABSORPTION RESULTS. SD IS THE STANDARD DEVIATION OF THE SURFACE HEIGHT

Sample	h (mm)	SD (mm)	$\bar{\epsilon}$	E_{abs} (kJ)
10 ppi	79.0	6.3	0.611	24.0
20 ppi	48.9	9.9	0.759	29.8
40 ppi	40.9	8.4	0.799	31.4

B. Pressure traces, wave speed, and impulse

Pressure transducers are the diagnostic used to measure the shock wave and foam response during a test. Figure 5 shows the comparison for a test (calibration) without foam and with 40 ppi foam for a pressure transducer located 19.1 cm above the end wall, or 1.3 cm below the top surface of the foam layer. Time zero is when the first pressure rise is observed. For the test without foam, a planar shock wave is observed from time zero to 0.75 ms, where a second pressure rise is observed due to the reflected shock from the end wall of the shock tube traveling vertically upwards. For the foam sample, a shock is not observed initially (no pressure discontinuity), however, there is a much greater increase in the pressure. This initial pressure rise is just below the level of the reflected pressure without foam which indicates a strong compression of the gas and foam in this region, nearly as much as would be observed at a rigid wall. The velocity of the upper surface of the foam layer is not measured; however, a reasonable assumption is that it moves with a velocity similar to the particle velocity of the gas behind the incident shock, 914 m/s. At this velocity the

foam deforms so quickly that by the time the pressure trace peaks for the first time (0.1 ms) the top surface of the foam has been compressed to a level below the transducer surface. A second peak in pressure of the foam test occurs at 0.64 ms and reaches a maximum of 14.5 MPa. This is approximately twice the maximum observed pressure without the foam which means the inertia of the foam compressing against the end wall of the shock tube has resulted in a stronger shock reflection; one whose pressure peak is very short lived, however.

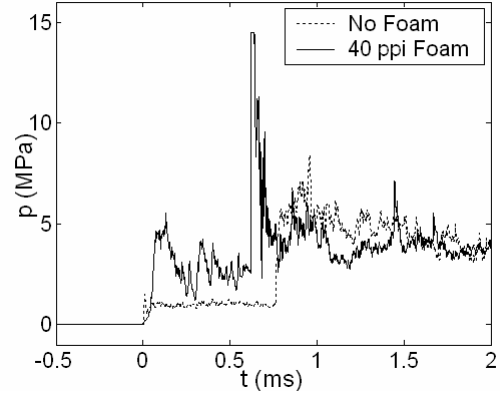


Figure 5. Pressure trace comparison.

Figure 6 shows the incident wave speed as it travels through the foam layer. The line represents the average shock wave speed for the experiment with no foam. The shock wave speed for the no foam experiment was 1,006 m/s and the average incident wave speeds (not shock waves) for the 40, 20, and 10 ppi samples were 206, 265, and 312 m/s, respectively. The change in wave speed varies dramatically from point to point for the 10 and 40 ppi experiments which make an “average” wave speed value somewhat questionable (especially considering that with a larger number of more closely spaced transducers the wave speed in the foam may be observed to slow over time and not just reach an average value); however, it is reasonable to conclude that the presence of the foam reduces the wave speed to approximately 25% of its initial value. The presence of a negative wave speed at the 10 cm location for the 40 ppi sample does not mean that the shock has reflected already; the transducer downstream has registered a reading before the upstream transducer, resulting in a negative velocity value--this may be due to some compression of the foam pushing against the face of the downstream transducer before the hydrodynamic shock wave has arrived.

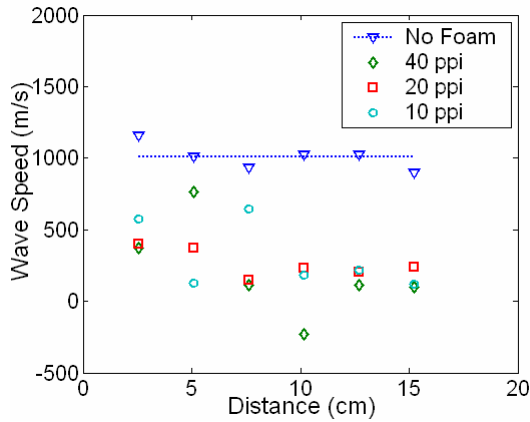


Figure 6. Wave speed in the foam layer; 0 cm is the top surface of the sample.

The impulse of the compressing foam on the end wall remains relatively constant for the three different foam materials. Impulse is calculated using the measured pressure from a transducer located just above the top surface of the foam layer and twice the amount of time it takes for the wave to travel from the top surface to the end wall. Impulse results for the 40, 20, and 10 ppi samples are 113, 133, and 107 N-s, while the interaction times are 1.56, 1.54, and 1.55 ms, respectively.

V. CONCLUSIONS

A series of open-cell Al foam samples have been studied in a shock tube as an initial validation database for code development on the shock mitigation characteristics of solid Flibe foam anticipated to be used in IFE Z-pinch reactor containment protection. Foams of the same porosity with three different cell sizes were studied with the smallest cell size foam having the greatest energy absorbing characteristics. The compression of the foam was found to be highly anisotropic, which is thought to be a result of structural variations within the foam volume, or localized shock focusing in the open-cell channels. The incident shock wave degenerated into a non-

discontinuous compression wave in the two-phase foam but resulted in greater peak pressures. The wave speed was reduced significantly as it passed through the foam and should provide a useful quantitative measure for benchmarking computer simulations for this material. Impulse calculations were insensitive to the pore size of the foam material but could be a factor for either larger or smaller pores than were tested. The current design of a conical, or piece-wise conical, RTL should be both structurally enhanced for installation purposes, and provide a large measure of energy absorption during the thermonuclear reaction, being filled with a solid metallic foam.

REFERENCES

- [1] R. Moir, "HYLIFE – II: A molten-salt inertial fusion energy power plant design-final report," *Fusion Technology*, Vol. 25, pp. 5-25 (1994).
- [2] C. Olson et al., "Development path for Z-pinch IFE," *Fusion Science and Technology*, Vol. 47, pp. 633-640 (2005).
- [3] K. Kitagawa, M. Yokoyama, M. Yasuhara, "Attenuation of shock waves by porous materials," 24th International Symposium on Shock Waves Proceedings, Beijing, China, Paper 2692 (2004).
- [4] M.H. Anderson, J.G. Oakley, P. Meekunnasombat, R. Bonazza, "The dynamics of a shock wave and aluminum foam layer interaction," 25th International Symposium on Shock Waves Proceedings, Bangalore, India, Paper 1197 (2005).
- [5] M.H. Anderson, B.P. Puranik, J.G. Oakley, P.W. Brooks, R. Bonazza, "Shock tube investigation of hydrodynamic issues related to inertial confinement fusion," Vol. 10, No. 5, pp. 377-387 (2000).
- [6] L.J. Gibson, M.F. Ashby, "Cellular solids, structure & properties," Pergamon Press, Oxford, 1988.
- [7] Energy Research and Generation, Inc. "Duocell Aluminum Foam Brochure," 900 Stanford Ave., Oakland, CA (510) 658-9785.
- [8] T.G. Nieh, K. Higashi, J. Wadsworth, "Effect of cell morphology on the compressive properties of open-cell foams," Vol. A283, pp. 105-110 (2000).
- [9] T.G. Nieh, J.H. Kinney, J. Wadsworth, A.J.C. Ladd, "Morphology and elastic properties of aluminum foam produced by a casting technique," *Scripta Materialia*, Vol. 38, No. 10, pp. 1487-1494 (1998).